ISSN 1028-334X, Doklady Earth Sciences, 2006, Vol. 407, No. 2, pp. 312–316. © Pleiades Publishing, Inc., 2006.
Original Russian Text © B.M. Koprov, S.V. Anisimov, V.M. Koprov, 2006, published in Doklady Akademii Nauk, 2006, Vol. 407, No. 1, pp. 96–101.

GEOPHYSICS

Variations in the Electric Field and Turbulence in the Surface Atmospheric Layer

B. M. Koprov[1], S. V. Anisimov[2], and V. M. Koprov[1]

Presented by Academician G.S. Golitsyn June 15, 2005

Received June 16, 2005

DOI: 10.1134/S1028334X0602036X

An experiment was carried out on the synchronous recording, in cloudless summer conditions in the middle region of Russia, of variations in the vertical component of electric field intensity E'; temperature; and the wind velocity components T', U', V', and W'. It was found that the correlation coefficient is positive between W' and E' and negative between U' and E'. If the temperature gradient sign changes to the opposite one, the correlation signs are retained, while the sign of the $T'-E'$ correlation changes to the opposite one. To a first approximation, this fact is explained by the advective transport of spatially similar fields of temperature and charge density formed near the surface. The temperature field gradient changes its direction from day to night, while the charge density gradient conserves its direction. The proposed model represents a relative variation of $\frac{E'}{\sigma_E}$ in the form of a linear function of relative variations in $\frac{U'}{\sigma_U}$, $\frac{V'}{\sigma_V}$, $\frac{W'}{\sigma_W}$, and $\frac{T'}{\sigma_T}$. We have found relations between the linear coefficients and experimental correlation coefficients.

1. The intensity of the electric field near the Earth has a regular vertical component (~100 V/m). Hereafter, when the terms "intensity" or "intensity of electric field" are used, it should be kept in mind that this term relates only to the vertical component. The stress generally decreases with height. The field is most variable near the surface mainly due to turbulent mixing of the near-surface atmosphere. Spatiotemporal variability of the field and its relation with turbulence are considered in [1–4]. The main attention was devoted to spectra of short-period variations and air electric structures associated with nonuniform distribution of the volume charge near the observation point [4, 5].

It is known that vertical turbulent heat flux is an important component of the heat balance at the surface. It is assumed that circulation cells, which realize this flux [6], also transport electric charges in a manner that is similar to how they transport various gas or aerosol admixtures. The direction of such transport does not depend on the direction of the heat flux but is determined only by the fact of whether or not the surface is the source of admixture or its sink [7–9].

Let q be the density of the charge, U the longitudinal component of wind velocity, V the component normal to the mean wind, and W the vertical component. All these values are functions of coordinates and time. The vertical turbulent charge flux Z can be determined from pulsation data in the following manner:

$$Z = \overline{W'q'}.$$

The prime here and below denotes variation of the corresponding value (i.e., deviation from the time mean) and the overbar is time averaging. The existing sensors of charge concentration are not applicable for pulsation measurements. At the same time, the intensity of electric field, which by definition is the force applied to a unit charge from all charges located at the surface and above it (i.e., in the atmosphere), is easily measured.

Since there is a correlation between the intensity of the field and the spatial distribution of the charge, which is determined by the Coulomb law, we can expect a positive correlation between the variations in intensity at the point of observation and charge concentration in the neighborhood of the point. Therefore, covariations of $\overline{W'E'}$ and $\overline{U'E'}$ provide information at least about the signs of covariations between $\overline{W'q'}$ and $\overline{U'q'}$, i.e., about the direction of the charge flux.

In order to investigate the statistical correlation between variations in velocity and temperature and

[1] *Oboukhov Institute of Atmospheric Physics, Russian Academy of Sciences, Pyzhevskii per. 3, Moscow, 109017 Russia*

[2] *Schmidt Joint Institute of Physics of the Earth, Russian Academy of Sciences, ul. Bol'shaya Gruzinskaya 10, Moscow, 123810 Russia*

variations in the intensity of the field, specialists from the Institute of Atmospheric Physics and the Institute of Physics of the Earth carried out a joint experiment in May–June 2004 at the test site of the Borok observatory in the Yaroslavl region.

2. Five sensors of the vertical component of field intensity E_1– E_5 (flux meters) were installed on the soil profile with a spacing of 5 m. Four thermometers T_1–T_4 (time constant of the sensors is 0.01 s) were located on the supports in the form of 2-m-high pillars along the profile parallel to the line of flux meters at a distance of 5 m. The thermometer was supplemented with a three-component acoustic anemometer installed on one of these supports [9] to measure the variations in the longitudinal, transversal, and vertical components of velocity in a frequency band of 0–16 Hz. Long-term synchronous records of all instruments were made with a sampling frequency of 16 Hz and 14-bit digitization of the signals. In this work, we limited ourselves to the analysis of the daytime and nighttime measurements in cloudless conditions. A pyranometer was used to control the cloud cover. During rain, fog, or dewfall, the measurements were not performed.

3. The statistical structure of the measured signals was studied by means of correlation and spectral analysis. In order to exclude the influence of the daily evolution of the measured values on the statistical characteristics of their variations, we determined the variations as deviations from running mean values over a time interval, which was usually taken equal to 20 min. The duration of realization usually exceeded 1 h. At a sampling frequency of 16 Hz, we could estimate the values of spectral densities in the frequency interval 0.001–8 Hz without notable systematic error and with sufficient statistical reliability. Intervals of records with a practically unchanged intensity of variations were chosen for the analysis. Since the Borok test site has a sufficiently long uniform surface (grass cover with a height not exceeding 10 cm), we considered that the conditions of horizontal uniformity and stationarity were observed. Under these conditions, we can consider that spatiotemporal correlation functions depend only on the difference of horizontal coordinates and time $\Delta x = x_2 - x_1$, $\Delta y = y_2 - y_1$, $\tau = t_2 - t_1$:

$$R_{ET} = \overline{E'(x_1, y_1, z_1, t_1)T'(x_2, y_2, z_2, t_2)} = R_{ET}(\Delta x, \Delta y, \tau),$$

$$R_{TT} = \overline{T'(x_1, y_1, z_1, t_1)T'(x_2, y_2, z_2, t_2)} = R_{TT}(\Delta x, \Delta y, \tau),$$

$$R_{EE} = \overline{E'(x_1, y_1, z_1, t_1)E'(x_2, y_2, z_2, t_2)} = R_{EE}(\Delta x, \Delta y, \tau).$$

Figure 1 shows autocorrelation functions $R_{TT}(\Delta x, \Delta y, \tau)$ and $R_{EE}(\Delta x, \Delta y, \tau)$ measured at equal spacings between the sensors $\Delta x = 5$, $\Delta y = 0$ (X-axis coincides with the line of flux meters, and the distances are given in meters). It is seen that time correlation radii are significantly different (approximately 10 s for the temperature field and 60 s for the intensity field). Spacing of the sensors led to a decrease in the maximum value of R_{TT} up to 0.6, whereas the maximum of function R_{EE} decreased only by 0.04. At the same time, the displacements of maxima τ_T and τ_E turned out to be similar. It is clear that the $\frac{\Delta x}{\tau_T}$ ratio is the rate of the displacement of temperature inhomogeneities along the line of sensors. The fact that this rate coincided with the $\frac{\Delta x}{\tau_E}$ value and the actual wind velocity along the base testifies to the horizontal displacement of the intensity field together with the air. This is possible only in the case of the displacements of inhomogeneities of the charge density field [10]. The difference between the correlation radii for the temperature and intensity fields is a consequence of the fact that intensity at the given point near the underlying surface is determined by the distribution of the charges in the entire half-space over this point.

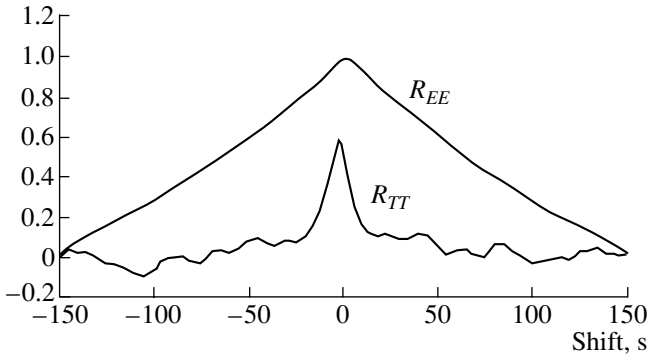

Fig. 1. Correlation functions $R_{EE}(\Delta x, 0, \tau)$ and $R_{TT}(\Delta x, 0, \tau)$ at unstable stratification and a distance between the corresponding sensor equal to $\Delta x = 5$ m.

In the spectral terminology, this difference between the correlation functions corresponds to a displacement of the energy-carrying interval of the intensity spectrum to the range of lower frequencies than in the spectra of temperature and wind velocity. The slopes of the power law intervals of temperature and velocity spectra in the frequency interval 0.003–8 Hz are close to –5/3, while approximation with –8/3 power law is more applicable for the spectrum of variations in the intensity range 0.001–0.1 Hz [10, 11]. Figure 2 shows autospectra of two components of velocity, temperature, and intensity.

Spectral correlation coefficients r_{ET}, r_{UT}, and r_{UE} for unstable (*4*, *5*, *6*) and stable (*1*, *2*, *3*) stratifications are shown in Fig. 3. As usual, we assume that the spectral

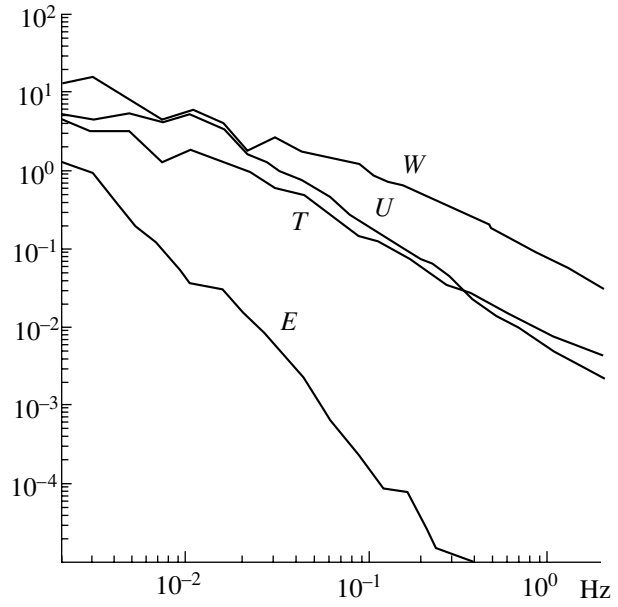

Fig. 2. Autospectra at unstable stratification (conventional units).

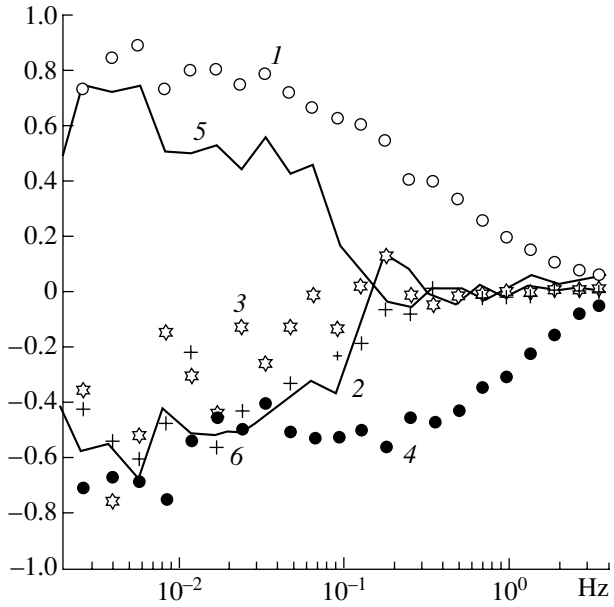

Fig. 3. Spectral correlation coefficients: stable stratification: (*1*) r_{UT}, (*2*) r_{ET}, (*3*) r_{UE}; unstable stratification: (*4*) r_{UT}, (*5*) r_{ET}, (*6*) r_{UE}.

correlation coefficient for processes $a(t)$ and $b(t)$ is the frequency function f determined by relation

$$R_{ab}(f) = \frac{c_{ab}(f)}{\sqrt{F_{aa}(f)F_{bb}(f)}},$$

where $c_{ab}(f)$ is the cospectrum of the processes considered here, and $F_{aa}(f)$ and $F_{bb}(f)$ are their autospectra.

As seen from Fig. 3, the spectral correlation coefficient r_{ET} is positive at unstable stratification and negative at stable stratification. At the same time, coefficient r_{UE} is negative at any stratification at frequencies lower than 0.1 Hz, while it turns to zero at frequencies greater than 0.1 Hz. According to the results of the analysis (not shown in Fig. 3), coefficient r_{WE} is positive at any stratification, and its value does not exceed 0.2.

4. The data presented in Fig. 3 characterize statistical correlations between field intensity variations, temperature, and longitudinal velocity component. We note that variations of E qualitatively correlate with U and W similarly to air temperature T at unstable stratification, when the heat flow is directed upward: the correlation between E and W is positive similarly to the correlation between T and W, while the correlation between E and U is negative similarly to the correlation between T and U. Detailed information about correlation coefficients between U, W, and T is given, for example, in a thorough study made in [12].

Let us consider a linear approximation, within which the relative variation of field intensity $\frac{E'}{\sigma_E}$ (σ_E is root-mean-square variation) is considered to be a linear function of relative variations of T, U, W, V, and A, where A characterizes the joint influence of additional factors not related statistically to wind and temperature:

$$\frac{E'}{\sigma_E} = \alpha\frac{T'}{\sigma_T} + \beta\frac{U'}{\sigma_U} + \gamma\frac{W'}{\sigma_W} + \delta\frac{V'}{\sigma_V} + \varepsilon\frac{A'}{\sigma_A}. \quad (1)$$

Sequentially multiplying (7) by $\frac{E'}{\sigma_E}, \frac{T'}{\sigma_T}, \frac{U'}{\sigma_U}, \frac{W'}{\sigma_W}$ and averaging the obtained relations under the assumption that

$$\overline{V'T'} = 0, \quad \overline{V'W'} = 0, \quad \overline{V'U'} = 0, \quad \overline{A'T'} = 0,$$
$$\overline{A'W'} = 0, \quad \overline{A'V'} = 0,$$

we get

$$\frac{\overline{E'^2}}{\sigma_E^2} = 1 = \alpha^2 + \beta^2 + \gamma^2 + \delta^2 + \varepsilon^2 + 2\alpha\beta R_{UT} + 2\alpha\gamma R_{WT} + 2\beta\gamma R_{UW}, \quad (2)$$

$$\frac{\overline{E'T'}}{\sigma_E\sigma_T} = R_{ET} = \alpha + \beta R_{UT} + \gamma R_{WT}, \quad (3)$$

$$\frac{\overline{E'U'}}{\sigma_E\sigma_U} = R_{UE} = \alpha R_{UT} + \beta + \gamma R_{UW}, \quad (4)$$

$$\frac{\overline{E'W'}}{\sigma_E\sigma_W} = R_{WE} = \alpha R_{WT} + \beta R_{UW} + \gamma. \quad (5)$$

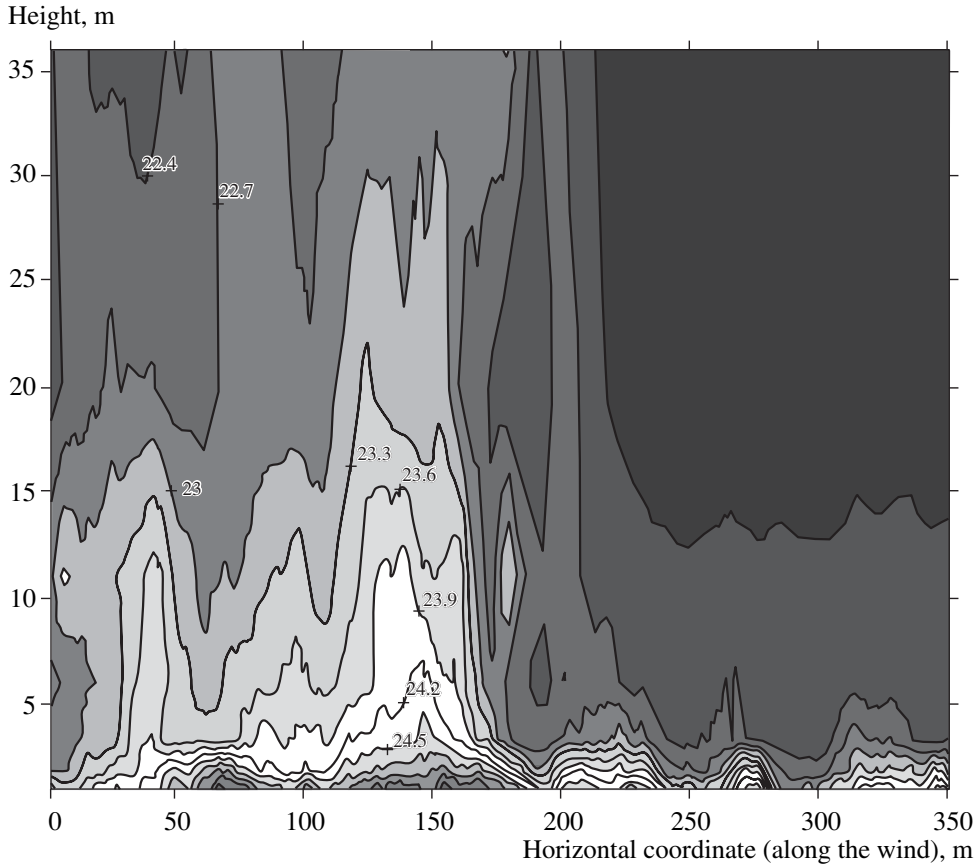

Fig. 4. Example of coherent structure in temperature field up to an altitude of 36 m.

It is easy to understand that it is only at $\alpha = 0$ that one can get correlations R_{ET}, R_{UE}, and R_{WE} of the signs, which correspond to Fig. 3, as well as the equality of their absolute values related to stable and unstable stratifications.

Applying the same assumption about linearity to spectral correlation coefficients and taking into account that $\alpha = 0$, we get, similarly to (8)–(11), the following:

$$1 = \beta^2 + \gamma^2 + \delta^2 + \varepsilon^2 + 2\beta\gamma r_{UW}, \quad (6)$$

$$r_{ET} = \beta r_{UT} + \gamma r_{WT}, \quad (7)$$

$$r_{UE} = \beta + \gamma r_{UW}, \quad (8)$$

$$r_{WE} = \beta r_{UW} + \gamma. \quad (9)$$

We assume that the linear coefficients considered here do not depend on frequency.

We get the following from (8) and (9):

$$\beta = \frac{r_{UE} - r_{UW} r_{WE}}{1 - r_{UW}^2}, \quad (10)$$

$$\gamma = \frac{r_{WE} - r_{UW} r_{UE}}{1 - r_{UW}^2}. \quad (11)$$

At $r_{UW} = -0.4$, $r_{UE} = -0.4$ (see Fig. 3) and $r_{WE} = 0.2$. Hence, $\beta = -0.4$ and $\gamma = 0.05$. Assuming for instability conditions $r_{UT} = -0.7$, $r_{WT} = 0.5$, we get from Eq. (7) the following estimate: $r_{ET} = 0.3$ (at stability $r_{ET} = -0.3$). These estimates have the necessary sign, but their absolute values are notably lower than the experimental ones. This can be related to the fact that, according to the experimental conditions, the field intensity and velocity components were observed not at one point but at a distance of 5 m along the horizontal direction and 2 m along the vertical direction. If we assume that $\beta = -0.6$, $\gamma = 0.16$, we get for unstable stratification $r_{ET} = 0.5$. Instead of (2) at $\alpha = 0$, we get $\beta^2 + \gamma^2 + \delta^2 + \varepsilon^2 + 2\beta\gamma r_{UW} = 1$. From this, we derive that $\sqrt{\delta^2 + \varepsilon^2} = 0.73$. Then, Eq. (1) takes the following form:

$$\frac{E'}{\sigma_E} = -0.6\frac{U'}{\sigma_U} + 0.16\frac{W'}{\sigma_W} + \delta\frac{V'}{\sigma_V} + \varepsilon\frac{A'}{\sigma_A}.$$

Thus, the uncorrelated terms V and A make the main contribution to the dispersion, and it is likely that the main part of this contribution is the contribution of V. Among the correlated terms, the greatest contribution to the dispersion of intensity variation belongs to the variations in the longitudinal velocity. If we assume

that $\alpha = 0$, we neglect the temperature dependence of the density of electric charges.

The observed variations and correlation between E and T in this approximation are explained by the similarity between the fields of charge and temperature and by their advective transport. If the surface is the source of two admixtures X and Y, which are not interrelated (in our case, this is temperature considered as passive admixture and charge), then concentration fields of X and Y are formed near the surface such that the cosine of the angle between vectors grad$X$ and grad$Y$ is everywhere close to unity. In other words, the surfaces of equal values of substances X and Y would have the same form. This also explains the high correlation observed between variations of concentrations of H_2O and CO_2 in the surface layer [8].

It is known that the main contribution to the vertical heat flux is made by coherent structures, this contribution being characterized by a synchronous and prolonged temperature increase in the whole surface layer by approximately σ_T [6, 13]. Such a structure is shown in Fig. 4 in the form of a chart of temperatures obtained from measurements at seven vertically separated points, reaching a height of 36 m. According to the supposition made earlier about the similarity of temperature and sign fields, the most significant changes in the charge density should occur during the propagation of such structures. As this takes place, the most significant variation in the intensity of the electric field at the surface will occur.

5. The materials presented here allow us to make the following conclusions.

A component caused by the nonuniform horizontal distribution of charge in the surface layer and the transport of this charge field by mean wind exists in the variations of the intensity of electric field near the underlying surface. The transport velocity of charge density inhomogeneities coincides with that of temperature inhomogeneities at a height of 2 m and is close to the wind velocity.

A positive correlation is observed between the variations in intensity and vertical wind velocity. Variations in field intensity and longitudinal wind show a negative correlation that does not depend on the sign of the stability parameter in the surface layer.

The correlation coefficient between field intensity and temperature is positive at unstable stratification and negative at stable stratification. The absolute value of this coefficient is close to 0.6.

Since the intensity of electric field at the surface is determined by the distribution of the charges over the surface. One can suppose that signs of WE and Wq covariations coincide. This implies that the turbulent mixing can generate charge flux, the direction of which remains unaltered during the whole day, in contrast to the turbulent heat flux that changes direction with change in sign of the stratification parameter.

ACKNOWLEDGMENTS

This work was supported by the Program of the Division of Earth Sciences of the Russian Academy of Sciences "Physics of the Atmosphere: Electrical Processes and Radiophysical Methods of Research."

REFERENCES

1. W. A. Hoppel, R. V. Anderson, and J. C. Willet, in *The Earth's Electrical Environment* (Nat. Acad. Press, Washington, 1986).
2. D. G. Yerg and K. R. Johnson, J. Geophys. Res. **79**, 2177 (1974).
3. S. V. Anisimov and E. A. Mareev, Dokl. Akad. Nauk **381**, 107 (2001) [Dokl. Earth Sci. **381**, 975 (2001)].
4. S. V. Anisimov, N. N. Shikhova, E. A. Mareev, and M. V. Shatalina, Izv. Ross. Akad. Nauk, Fiz. Atmosf. Okeana **39**, 766 (2003).
5. S. V. Anisimov and E. A. Mareev, Dokl. Akad. Nauk **371**, 101 (2000) [Dokl. Earth Sci. **371**, 369 (2001)].
6. B. M. Koprov, V. M. Koprov, and T. I. Makarova, Boundary-Layer Meteorol. **111**, 19 (2003).
7. N. F. Elansky, B. M. Koprov and D. Yu. Sokolov, Izv. Ross. Akad. Nauk, Fiz. Atmosf. Okeana **31**, 109 (1995).
8. Yu. A. Volkov, L. G. Elagina, V. V. Kudryavtsev, et al., Izv. Ross. Akad. Nauk, Fiz. Atmosf. Okeana **24**, 805 (1988).
9. L. G. Elagina, B. M. Koprov, and D. F. Timanovsky, Izv. Ross. Akad. Nauk, Fiz. Atmosf. Okeana **14**, 926 (1978).
10. S. V. Anisimov, E. A. Mareev, N. M. Shikhova, and E. M. Dmitriev, Geophys. Res. Lett. **29**, 2217 (2002).
11. S. V. Anisimov, E. A. Mareev, and V. Yu. Trakhtenherz, Geomagn. Aeronomy **31**, 669 (1991).
12. B. A. Kader and A. M. Yaglom, J. Fluid Mech. **212**, 637 (1990).
13. B. M. Koprov, V. M. Koprov, and T. I. Makarova, Izv. Ross. Akad. Nauk, Fiz. Atmosf. Okeana **36**, 44 (2000).